Staphylococcal sRNA IsrR down-regulates methylthiotransferase MiaB under iron-deficient conditions

Maxime Barrault*, Elise Leclair*, and Philippe Bouloc[#]

Université Paris-Saclay, CEA, CNRS, Institute for Integrative Biology of the Cell (I2BC), 91198 Gif-sur-Yvette, France

N° ORCID:

- Maxime Barrault: 0000-0003-3949-7598
- Elise Leclair: 0009-0000-3706-6554
- Philippe Bouloc: 0000-0003-4601-3387

*Contributed equally.

[#]Correspondence: philippe.bouloc@i2bc.paris-saclay.fr

Running title: Staphylococcal sRNA IsrR down-regulates *miaB*.

Keywords: *Staphylococcus aureus*, IsrR, iron homeostasis, [Fe-S] clusters, small regulatory RNA, translational regulation.

ABSTRACT

Staphylococcus aureus is a major contributor to bacterial-associated mortality, owing to its exceptional adaptability across diverse environments. Iron, vital for most organisms, poses toxicity risks in excess. To manage iron, *S. aureus*, like many pathogens, employs intricate systems. We have recently identified IsrR as a key regulatory RNA induced during iron starvation. Its role is to curtail the synthesis of non-essential iron-containing proteins under iron-depleted conditions. In this study, we unveil IsrR's regulatory action on MiaB, an enzyme responsible for methylthio group addition to specific sites on transfer RNAs (tRNAs). We use predictive tools and reporter fusion assays to demonstrate IsrR's binding to the Shine-Dalgarno sequence of *miaB* RNA, thereby impeding its translation. The effectiveness of IsrR hinges on the integrity of a specific C-rich region. As MiaB is non-essential and contains two [4Fe-4S] clusters, IsrR induction spares iron by downregulating *miaB*. This likely enhances *S. aureus* fitness and aids in navigating the host's nutritional immune defenses.

IMPORTANCE

In numerous biotopes, including those found within an infected host, bacteria confront the challenge of iron deficiency. They employ various strategies to adapt to this scarcity of nutrients, one of which involves the regulation of iron-containing proteins through the action of small regulatory RNAs. In our study, we demonstrate how IsrR, a small RNA from *S. aureus*, inhibits the translation of MiaB, a tRNA-modifying enzyme containing [Fe-S] clusters. Through this illustration, we shed light on a novel substrate for a small RNA sparing iron, thereby unveiling a way by which bacteria conserve their iron resource.

INTRODUCTION

Staphylococcus aureus is the leading cause of bacteria-associated mortality worldwide (1). Its pathogenicity is due to its adaptability across various biotopes and the expression of multiple virulence determinants. Iron is a trace element universally required for growth, but toxic in excess. *S. aureus*, akin to other pathogens, possesses elaborate systems for maintaining its intracellular iron homeostasis to match environmental conditions (2).

We recently identified and characterized IsrR, a regulatory RNA of *S. aureus*, contributing to an adaptive response to iron scarcity (3). By restricting non-essential iron-containing protein synthesis, IsrR spares iron for indispensable functions. *isrR* expression is repressed by the ferric uptake regulator (Fur) which is active in iron-rich environments. Induced during iron deficiency, IsrR targets Shine-Dalgarno motifs on mRNAs coding for iron-containing proteins, notably restraining translation of specific mRNAs (*fdhA*, *narG*, *nasD*, and *gltB2*) linked to nitrate respiration and encoding [Fe-S] cluster-dependent enzymes. Given the limited iron demands, fermentative pathways gain favor under limited iron conditions. IsrR is a functional analog from *E. coli* RyhB (4) and of other sRNAs found in diverse bacterial species (reviewed in (5, 6)) sharing targets and iron regulation. These similarities highlight a common evolutionary pressure, although IsrR is not an ortholog of these sRNAs, hinting at convergent evolution.

Hosts prevent pathogen growth through an arsenal of defense mechanisms, one of which, known as nutritional immunity, is the sequestration of nutrients such as iron (7). We reported that IsrR deficiency results in reduced virulence of *S. aureus* in a murine infection model, highlighting the role of IsrR in facilitating optimal spread of *S. aureus* in the host environment, probably critical for evasion of nutritional immunity (3).

Here, we demonstrate that IsrR downregulates *miaB* encoding a non-essential protein containing [Fe-S] clusters. This new example shows that IsrR is a central player in the maintenance of iron homeostasis in *S. aureus*.

MATERIALS AND METHODS

Bacterial strains, plasmids and growth conditions

Bacterial strains, plasmids and primers used for this study are described in Table 1. Plasmids were engineered by Gibson assembly (8) in *Escherichia coli* IM08B (9) as described (Table 1), using the indicated appropriate primers for PCR amplification. Plasmids were verified by DNA sequencing and then transferred into *S. aureus*.

S. aureus strains were grown aerobically in Brain Heart Infusion (BHI) broth at 37°C. *E. coli* strains were grown aerobically in Luria-Bertani (LB) broth at 37°C. Antibiotics were added to media as needed: ampicillin 100 µg/ml and chloramphenicol 20 µg/ml for *E. coli*; chloramphenicol 5 µg/ml and kanamycin 60 µg/ml for *S. aureus*. Iron-depleted media was obtained by the addition of DIP (2,2'-dipyridyl) 0.5 mM incubated for 30 min prior to any use.

Biocomputing analysis

Pairing predictions between IsrR and the mRNA targets were made using IntaRNA (10) set with default parameters except for suboptimal interaction overlap set to "can overlap in both". The sequences used for IsrR and mRNA targets were extracted from the *S. aureus* NCTC8325 strain (NCBI RefSeq NC_007795.1). For the mRNA targets, the sequences used started at the TSS when known (e.g., EMOTES (11) or were arbitrarily made to start at nucleotide -60 with respect to the +1 of translation. The sequences contain the 5' UTR and the 17 first codons of the CDS. Statistical analysis were made using a t-test. Error bars represent the 95% confidence interval following a Student's test.

Western blot analysis

The chromosomal *miaB-flag* reporter gene was constructed as described (Table 1). Strains were grown overnight with and without DIP. Protein extracts were prepared as follows: 4 mL of the bacterial culture were harvested by centrifugation at 4°C and 4500 RPM for 5 minutes. The resulting pellet was resuspended in 400 µL of 50 mM Tris-HCl. Cell disruption was achieved using a Fast-Prep homogenizer (MP Biomedicals). After disruption, protein extracts were obtained by centrifugation at 4°C and 15000 RPM for 15 minutes. The protein concentration of each extract was determined using the Bradford protein assay method. Ten µg of each protein extract were loaded onto a NuPAGE 4%-12% Bis-Tris gel. Electrophoresis was carried out at 150V for 45 minutes. Proteins were transferred from the gel to a PVDF membrane using the iBind system (Invitrogen). Immunolabeling was performed overnight with a rabbit anti-Flag antibody. After incubation with the primary antibody, an anti-rabbit IgG HRP-conjugated antibody (Promega) was used for detection. The iBlot system (Invitrogen) was employed for antibody incubation. Images of the immunolabeled membrane were acquired using a ChemiDoc MP imaging system (Bio-Rad).

Fluorescent translational reporter assay

A *miaB* translational reporter (P_{sarA}-5'miaB-mAm) was inserted between genes *SAOUHSC_00037* and *SAOUHSC_00039* in HG003 and HG003 Δ*isrR*::*tag135* using pRN112-5'miaB (Table 1), a pRN112 derivative, as described (12). Notably, the mAmetrine reporter gene (*mAm*) was placed in-frame and downstream *miaB* 18th codon with the *miaB* 5'UTR placed under the control of the P1 promoter of *sarA* ($P1_{sarA}$). Subsequently, the strains carrying the reporter fusion were transformed with plasmids expressing *isrR*, along with its various derivatives featuring CRR deletions. These plasmids are pRMC2ΔR-IsrR, pRMC2ΔR-IsrRΔC1, pRMC2ΔR-IsrRΔC2, pRMC2ΔR-IsrRΔC3, pRMC2ΔR-IsrRΔC1C2, pRMC2ΔR-IsrRΔC1C3, pRMC2ΔR-IsrRΔC2C3, and pRMC2ΔR-IsrRΔC1C2C3. For fluorescence measurements, the transformed strains were cultured overnight in BHI medium supplemented with chloramphenicol and DIP. Subsequently, cultures were washed three times with 1x phosphate-buffered saline (PBS). Fluorescence levels were quantified using a microplate reader (CLARIOstar) with excitation at 425 nm and emission at 525 nm. To ensure accuracy, fluorescence measurements were normalized by subtracting the auto-fluorescence of the HG003 strain (lacking the reporter construct), and all cultures were adjusted to an optical density at 600 nm (OD_{600}) of 1.

RESULTS

MiaB is a putative IsrR-target

We used CopraRNA (13), a software designed for predicting targets of bacterial sRNAs across diverse species, to unveil potential targets of IsrR. Given its conservation throughout the Staphylococcus genus, CopraRNA emerged as an efficient tool for IsrR target prediction, resulting in the successful validation of four of its targets as reported (3). Among the predicted targets, was the *miaB* messenger RNA (3, 14). The latter encodes MiaB, a methylthiotransferase catalyzing the addition of a methylthio group (ms^2) to isopentenyl adenine (i^6A) at position 37 (ms^2i^6A-37) of transfer RNA (tRNA) anticodons (15). This modification present in most tRNAs reading codons starting with a U is conserved from bacteria to human (16) contributing to stabilizes the codon–anticodon interaction (17) and affects translational accuracy (18).

To substantiate the proposed interaction between IsrR and *miaB* mRNA, we use the IntaRNA software (10). Our inputs were the complete IsrR sequence and the *miaB* 5' untranslated region (UTR) with 25 codons. IsrR is characterized by three single-stranded C-rich regions, denoted as CRR1, CCR1, and CRR3 (3). These sequences are common features among Firmicutes' regulatory RNAs binding to mRNAs (19). IntaRNA analysis indicated the potential pairing of IsrR with the Shine-Dalgarno sequence of the *miaB* RNA (Figure 1). The pairing involves 55 nucleotides, a significant energy of a predicted RNA-RNA score of -22.33 kcal/mol and the GCCCG of CCR3 being likely the seed motif of the interaction.

IsrR-dependent reduction of MiaB expression

To explore the potential influence of IsrR on *miaB* expression, a gene fusion was constructed wherein the native *miaB* gene was replaced by a copy harboring the complete *miaB* open reading frames extended with a C-terminal Flag sequence (Figure 2A). The resulting MiaB-Flag fusion protein was detectable through anti-Flag antibodies, thereby serving as a quantifiable surrogate for wild-type gene expression levels. This reporter fusion was integrated into the chromosomes of both HG003 and its corresponding Δ*isrR*::*tag135* isogenic derivative. Western blot analyses conducted on HG003 cultures cultivated under nutrient-rich conditions unveiled an unaltered MiaB-Flag abundance, irrespective of the presence or absence of *isrR*. This status quo was in line with the known Fur-mediated repression of *isrR* under iron-replete conditions. However, introducing the iron chelator 2,2'-dipyridyl (DIP) into the growth medium elicits a release from Fur repression, consequently inducing IsrR expression (3). Remarkably, under DIP-induced conditions, no MiaB-Flag was detected regardless of the *isrR* background (Figure 2B). This result is interpreted as iron depletion leading to apo-MiaB being unstable. To overcome this issue, a *fur*::tet allele (20) was introduced by phage-mediated transduction in

the *miaB-flag* and Δ*isrR miaB-flag* strains rendering *isrR* constitutively expressed (3). Expectedly, in this genetic background, MiaB-Flag was barely visible in the *fur* strain as opposed to its *fur* Δ*isrR* derivative (Figure 2C).

IsrR-mediated post-transcriptional regulation of *miaB* expression

In the absence of Fur, *isrR* is expressed and *miaB* is downregulated; the observation is explained by the base pairing interaction between IsrR and *miaB* RNA, putatively inhibiting *miaB* RNA translation. To examine this hypothesis, a genetic reporter system, based on pRN112 (12), was constructed wherein the 5' untranslated region (5'UTR) of *miaB*, along with an additional 54 nucleotides, was cloned under the transcriptional control of the P1 *sarA* promoter ($P1_{sarA}$) (Figure 3A). Furthermore, to monitor the translation from this leader sequence, the mAmetrine gene (*mAm*) was inserted in-frame downstream of this sequence. The resulting fluorescence served as a proxy for *miaB* expression levels independently of its transcriptional regulation. To mitigate concerns associated with multi-copy reporter plasmids, the $P1_{sarA}$*miaB*_5'UTR*mAm* construct was integrated into the chromosome of both HG003 strain and its *isrR*::*tag135* derivative. As for the endogenous *miaB*, the 5'UTR*miaB*-mAm reporter exhibited significant downregulation under iron-starved conditions in an IsrR-dependent manner, while its transcription was driven from $P1_{sarA}$ (Figure 3B). Our experimental findings conclusively demonstrate that IsrR exerts its regulatory influence at the translational level.

The C-rich region 3 (CRR3) of IsrR plays a pivotal role in the downregulation of *miaB* mRNA.

Pairing interactions between sRNAs and their targets are initiated by a kissing complex between single-stranded regions, which then propagates within both partners (21). sRNAs can have multiple seed regions, usually C-rich in *S. aureus* (19), specific to given targets as exemplified by RNAIII (review in (22)) or with redundant activities as in RsaE (23). To determine specific regions of IsrR responsible for its regulatory activity against *miaB* mRNA, experiments using the HG003 Δ*isrR*::*tag135* strain, harboring the 5'UTR *miaB* fluorescent reporter were conducted. Plasmids expressing various IsrR derivatives, including wild-type IsrR, IsrR lacking CRR1, CRR2, CRR3, or all three CRRs were used. *isrR* was placed under the control of the *tet* promoter (P_{tet}) in the absence of the Tet repressor (TetR), although it should be noted that a Fur binding site is present within the transcribed sequence (3). Consequently, we supplemented the growth media with DIP to prevent an Fur repression on *isrR* expression.

The presence of a plasmid expressing IsrR markedly diminished the fluorescence of the reporter fusion when compared to a control plasmid or a plasmid expressing IsrR with no CRR

motif. In contrast, the deletion of CRR3 resulted in a significant increase in mAmetrine fluorescence. However, the deletion of CRR1 and CRR2 in isolation had no substantial impact on IsrR's activity against the *miaB* 5'UTR reporter (Figure 3C). This observation suggests that these two motifs may either be dispensable for the regulatory activity or possess redundant functions with respect to the *miaB* 5'UTR.

To discern between these possibilities, we introduced into the Δ*isrR*::*tag135* strain plasmids expressing different *isrR* derivatives with deletions of two CRRs. As expected, strains carrying alleles with the CRR3 deletion (*isrR*ΔC1C3 and *isrR*ΔC2C3) failed to complement the Δ*isrR* allele. In contrast, *isrR*ΔC1C2 was still capable of downregulating the fluorescence of the P_{sarA}*miaB*_5'UTR*mAm* reporter (Figure 3C). These findings align with the results obtained from IntaRNA analysis, which indicates that the *IsrR*/*miaB* mRNA pairing energy remains substantial as long as CRR3 and its surrounding region remain intact (Figure 1).

It is worth noting that the requirement for CRRs in IsrR activity appears to be contingent upon its target mRNA (Figure 4). For instance, the absence of CRR3 does not impede the downregulation of *gltB2* and *fdhA* mRNAs (3). Conversely, for the latter mRNAs, the integrity of both CRR1 and CRR2 is indispensable, presenting a contrast to *miaB* mRNA regulation. This observation suggests that the acquisition of multiple CRRs, together with their adjacent regions, confers on regulatory RNAs the ability to control a wider range of target mRNAs. sRNAs likely evolve by acquiring new domains to interact with different targets (*e.g. miaB* RNA vs *gltB2* mRNA). At the same time, mRNAs may evolve to adapt to the sRNA motifs that are available (*e.g. gltB2* RNA vs *fdhA* mRNA).

DISCUSSION

The relationship between iron metabolism and the MiaB enzyme has been a subject of scientific interest for several decades. As far back as the 1960s, researchers noted the absence of certain tRNA modifications in *E. coli* cultured in iron-free media, underscoring the connection between iron availability and tRNA modifications (24). Subsequent investigations revealed that the *miaB* gene encodes the tRNA methylthiotransferase responsible for these modifications, and mutations in *miaB* were found to reduce decoding efficiencies under specific conditions (15). Notably, MiaB contains two [4Fe-4S] clusters, and under iron-starved conditions, these clusters become depleted, rendering MiaB inactive (25). Furthermore, as shown here, in iron-starved condition, MiaB-Flag was not detectable suggesting that in the absence of iron cluster, MiaB is degraded.

In *E. coli*, MiaB's influence extends to the regulation of Fur through a distinctive mechanism (26). The *fur* gene is preceded by *uof*, an open reading frame located "upstream of fur", and the translation of *fur* is tightly coupled to that of *uof*. An intriguing aspect of this regulatory relationship is the presence of a codon UCA, decoded by a MiaB-dependent $tRNA^{Ser}$. Consequently, efficient *uof*/*fur* translation relies on functional MiaB. When iron-starvation conditions prevail, MiaB becomes inactive, impairing tRNA methylthiolation. This, in turn, leads to reduced *uof*/*fur* translation, ultimately favoring the expression of iron uptake genes. However, this regulation is not conserved in *S. aureus* since no *uof*-like sequence was observed.

In standard laboratory conditions, Enterobacteria appear to be resilient to the absence of MiaB (27). Despite limited knowledge regarding MiaB in staphylococci, similar trends are observed in other bacterial species, where MiaB is not essential (28). Consequently, inhibiting MiaB synthesis is likely to have minimal or no discernible consequences in various growth conditions. Since MiaB relies on [Fe-S] clusters as cofactors, suppressing its synthesis in iron-starved environments spares iron, allowing it to be redirected toward essential cellular processes.

This iron conservation strategy is exemplified by IsrR in *S. aureus*, which prevents *miaB* translation upon induction in iron-depleted conditions, thus likely contributing to improved bacterial fitness. Notably, inhibition of *miaB* RNA translation by a sRNA associated with the iron-sparing response is a novel feature that has not been reported in other organisms than *S. aureus* to date.

ACKNOWLEDGMENTS

This work was funded by the *Agence Nationale pour la Recherche* (ANR) ANR grant [ANR-19-CE12-0006-01 (sRNA-RRARE)] and by the *OI Microbes* from the *Université Paris-Saclay*. MB was the recipient of fellowships from the *Ministère de l'enseignement supérieur et de la recherche*. We thank our lab colleagues and Dos Equis for helpful discussions and warm support.

REFERENCES

1. Collaborators GBDAR. 2023. Global mortality associated with 33 bacterial pathogens in 2019: a systematic analysis for the Global Burden of Disease Study 2019. Lancet 400:2221-2248.

2. Sheldon JR, Laakso HA, Heinrichs DE. 2016. Iron acquisition strategies of bacterial pathogens. Microbiol Spectr 4.

3. Coronel-Tellez RH, Pospiech M, Barrault M, Liu W, Bordeau V, Vasnier C, Felden B, Sargueil B, Bouloc P. 2022. sRNA-controlled iron sparing response in Staphylococci. Nucleic Acids Research 50:8529-8546.

4. Masse E, Gottesman S. 2002. A small RNA regulates the expression of genes involved in iron metabolism in *Escherichia coli*. Proc Natl Acad Sci U S A 99:4620-5.

5. Chareyre S, Mandin P. 2018. Bacterial iron homeostasis regulation by sRNAs. Microbiol Spectr 6.

6. Oglesby-Sherrouse AG, Murphy ER. 2013. Iron-responsive bacterial small RNAs: variations on a theme. Metallomics 5:276-86.

7. Murdoch CC, Skaar EP. 2022. Nutritional immunity: the battle for nutrient metals at the host-pathogen interface. Nat Rev Microbiol 20:657-670.

8. Gibson DG. 2011. Enzymatic assembly of overlapping DNA fragments. Methods in Enzymology 498:349-61.

9. Monk IR, Tree JJ, Howden BP, Stinear TP, Foster TJ. 2015. Complete bypass of restriction systems for major *Staphylococcus aureus* lineages. MBio 6:e00308-15.

10. Mann M, Wright PR, Backofen R. 2017. IntaRNA 2.0: enhanced and customizable prediction of RNA-RNA interactions. Nucleic Acids Research 45:W435-W439.

11. Prados J, Linder P, Redder P. 2016. TSS-EMOTE, a refined protocol for a more complete and less biased global mapping of transcription start sites in bacterial pathogens. BMC Genomics 17:849.

12. de Jong NW, van der Horst T, van Strijp JA, Nijland R. 2017. Fluorescent reporters for markerless genomic integration in *Staphylococcus aureus*. Sci Rep 7:43889.

13. Wright PR, Georg J, Mann M, Sorescu DA, Richter AS, Lott S, Kleinkauf R, Hess WR, Backofen R. 2014. CopraRNA and IntaRNA: predicting small RNA targets, networks and interaction domains. Nucleic Acids Research 42:W119-23.

14. Mader U, Nicolas P, Depke M, Pane-Farre J, Debarbouille M, van der Kooi-Pol MM, Guerin C, Derozier S, Hiron A, Jarmer H, Leduc A, Michalik S, Reilman E, Schaffer M, Schmidt F, Bessieres P, Noirot P, Hecker M, Msadek T, Volker U, van Dijl JM. 2016. *Staphylococcus aureus* transcriptome architecture: from laboratory to infection-mimicking conditions. PLoS Genet 12:e1005962.

15. Esberg B, Leung HC, Tsui HC, Bjork GR, Winkler ME. 1999. Identification of the *miaB* gene, involved in methylthiolation of isopentenylated A37 derivatives in the tRNA of *Salmonella typhimurium* and *Escherichia coli*. Journal of Bacteriology 181:7256-65.

16. Grosjean H, Nicoghosian K, Haumont E, Soll D, Cedergren R. 1985. Nucleotide sequences of two serine tRNAs with a GGA anticodon: the structure-function relationships in the serine family of *E. coli* tRNAs. Nucleic Acids Research 13:5697-706.

17. Lim VI. 1997. Analysis of interactions between the codon-anticodon duplexes within the ribosome: their role in translation. Journal of Molecular Biology 266:877-90.

18. Bouadloun F, Srichaiyo T, Isaksson LA, Bjork GR. 1986. Influence of modification next to the anticodon in tRNA on codon context sensitivity of translational suppression and accuracy. Journal of Bacteriology 166:1022-7.

19. Geissmann T, Chevalier C, Cros MJ, Boisset S, Fechter P, Noirot C, Schrenzel J, Francois P, Vandenesch F, Gaspin C, Romby P. 2009. A search for small noncoding RNAs in *Staphylococcus aureus* reveals a conserved sequence motif for regulation. Nucleic Acids Res 37:7239-57.

20. Horsburgh MJ, Ingham E, Foster SJ. 2001. In *Staphylococcus aureus*, Fur is an interactive regulator with PerR, contributes to virulence, and Is necessary for oxidative stress resistance through positive regulation of catalase and iron homeostasis. J Bacteriol 183:468-75.

21. Tomizawa J. 1984. Control of ColE1 plasmid replication: the process of binding of RNA I to the primer transcript. Cell 38:861-70.

22. Felden B, Vandenesch F, Bouloc P, Romby P. 2011. The *Staphylococcus aureus* RNome and its commitment to virulence. PLoS Pathog 7:e1002006.

23. Rochat T, Bohn C, Morvan C, Le Lam TN, Razvi F, Pain A, Toffano-Nioche C, Ponien P, Jacq A, Jacquet E, Fey PD, Gautheret D, Bouloc P. 2018. The conserved regulatory RNA RsaE down-regulates the arginine degradation pathway in *Staphylococcus aureus*. Nucleic Acids Res 46:8803-8816.

24. Rosenberg AH, Gefter ML. 1969. An iron-dependent modification of several transfer RNA species in *Escherichia coli*. Journal of Molecular Biology 46:581-4.

25. Hernandez HL, Pierrel F, Elleingand E, Garcia-Serres R, Huynh BH, Johnson MK, Fontecave M, Atta M. 2007. MiaB, a bifunctional radical-S-adenosylmethionine enzyme involved in the thiolation and methylation of tRNA, contains two essential [4Fe-4S] clusters. Biochemistry 46:5140-7.

26. Vecerek B, Moll I, Blasi U. 2007. Control of Fur synthesis by the non-coding RNA RyhB and iron-responsive decoding. EMBO J 26:965-75.

27. Esberg B, Bjork GR. 1995. The methylthio group (ms2) of N6-(4-hydroxyisopentenyl)-2-methylthioadenosine (ms2io6A) present next to the anticodon contributes to the decoding efficiency of the tRNA. Journal of Bacteriology 177:1967-75.

28. Fey PD, Endres JL, Yajjala VK, Widhelm TJ, Boissy RJ, Bose JL, Bayles KW. 2013. A genetic resource for rapid and comprehensive phenotype screening of nonessential *Staphylococcus aureus* genes. mBio 4:e00537-12.

29. Herbert S, Ziebandt AK, Ohlsen K, Schafer T, Hecker M, Albrecht D, Novick R, Gotz F. 2010. Repair of global regulators in *Staphylococcus aureus* 8325 and comparative analysis with other clinical isolates. Infect Immun 78:2877-89.

Table 1; Strains, plasmids, and DNA primers used in this study.

Strains		
Name	*Background/genotype*	*Reference or construction*
HG003	as NCTC8325 *rsbU* and *tcaR* repaired	(29)
SAPhB1231	as HG003 Δ*isrR*::*tag135*	(3)
SAPhB1542	As HG003 *fur*::*tet*	(3)
SAPhB2338	as HG003 $P1_{sarA}$_5'UTR *miaB*::*mAm* (integrated downstream of *sqr*)	HG003 + pRN112-5'miaB
SAPhB2339	as HG003 $P1_{sarA}$_5'UTR *miaB*::*mAm* (integrated downstream of *sqr*) Δ*isrR*::*tag135*	SAPhB1231+ pRN112-5'miaB
SAPhB2351	as HG003 $P1_{sarA}$_5'UTR *miaB*::*mAm* (integrated downstream of *sqr*) Δ*isrR*::*tag135* pRMC2ΔR-IsrR	SAPhB2339 + pRMC2ΔR-IsrR
SAPhB2352	as HG003 $P1_{sarA}$_5'UTR *miaB*::*mAm* (integrated downstream of *sqr*) Δ*isrR*::*tag135* pRMC2ΔR-IsrRΔC1C2C3	SAPhB2339 + pRMC2ΔR-IsrRΔC1C2C3
SAPhB2353	as HG003 $P1_{sarA}$_5'UTR *miaB*::*mAm* (integrated downstream of *sqr*) Δ*isrR*::*tag135* pRMC2ΔR-IsrRΔC1	SAPhB2339 + pRMC2ΔR-IsrRΔC1
SAPhB2354	as HG003 $P1_{sarA}$_5'UTR *miaB*::*mAm* (integrated downstream of *sqr*) Δ*isrR*::*tag135* pRMC2ΔR-IsrRΔC2	SAPhB2339 + pRMC2ΔR-IsrRΔC2
SAPhB2355	as HG003 $P1_{sarA}$_5'UTR *miaB*::*mAm* (integrated downstream of *sqr*) Δ*isrR*::*tag135* pRMC2ΔR-IsrRΔC3	SAPhB2339 + pRMC2ΔR-IsrRΔC3
SAPhB2356	as HG003 $P1_{sarA}$_5'UTR *miaB*::*mAm* (integrated downstream of *sqr*) Δ*isrR*::*tag135* pRMC2ΔR-IsrRΔC1C2	SAPhB2339 + pRMC2ΔR-IsrRΔC1C2
SAPhB2357	as HG003 $P1_{sarA}$_5'UTR *miaB*::*mAm* (integrated downstream of *sqr*) Δ*isrR*::*tag135* pRMC2ΔR-IsrRΔC1C3	SAPhB2339 + pRMC2ΔR-IsrRΔC1C3
SAPhB2358	as HG003 $P1_{sarA}$_5'UTR *miaB*::*mAm* (integrated downstream of *sqr*) Δ*isrR*::*tag135* pRMC2ΔR-IsrRΔC2C3	SAPhB2339 + pRMC2ΔR-IsrRΔC2C3
SAPhB2366	as HG003 *miaB-flag*	HG003 + pIMmiaBflag
SAPhB2367	as HG003 *miaB-flag, Δisr*R::*tag135*	SAPhB1231+ pIMmiaBflag
SAPhB2374	as HG003 *miaB-flag, fur*::*tet*	SAPhB2366 + ϕ80 on SAPhB1542
SAPhB2376	as HG003 *miaB-flag, fur*::*tet*, Δ*isrR*::*tag135*	SAPhB2367+ ϕ80 on SAPhB1542

Plasmids		
Name	*Relevant properties*	*Reference or construction**
pRN112	pJB28-NWMN29-30 + $P1_{SarA}$-mAmetrine	(12)

pRN112-5'miaB	Chromosomal integration of the $P1_{sarA}$-5'miaB-mAm gene fusion between SAOUHSC_00037 and SAOUHSC_00039	2600/2906 on pRN112 + 3189/3190 on HG003
pIMAY	Chromosome engineering	(9)
pIMmiaBflag	*miaB* gene replacement with *miaB-flag*	1536/1537 on pIMAY + 3229/3230 and 3231/3232 on HG003
pRMC2ΔR	pRMC2 derivative with a tetR deletion. Constitutive expression from P_{tet}	(Coronel-Tellez*, et al.*, 2022
pRMC2ΔR-IsrRΔC1	Constitutive expression of *isrR*ΔC1	(3)
pRMC2ΔR-IsrRΔC2	Constitutive expression of *isr*RΔC2	(3)
pRMC2ΔR-IsrRΔC3	Constitutive expression of *isrR*ΔC3	(3)
pRMC2ΔR-IsrRΔC1C2	Constitutive expression of *isrR*ΔC1C2	(3)
pRMC2ΔR-IsrRΔC2C3	Constitutive expression of *isrR*ΔC2C3	2789/2790 on pRMC2ΔR-IsrRΔC2
pRMC2ΔR-IsrRΔC1C3	Constitutive expression of *isrR*ΔC1C3	2667/2668 on pRMC2ΔR-IsrRΔC1
pRMC2ΔR-IsrRΔC1C2C3	Constitutive expression of *isrR*ΔC1C2C3	2789/2790 on pRMC2ΔR-IsrRΔC1C2

Primers

Name	Sequence
1536	GGTACCCAGCTTTTGTTCCCTTTAGTGAGG
1537	GAGCTCCAATTCGCCCTATAGTGAGTCG
2600	TTAGTTAATTATAACTAATTAAAAATGAGAAGTAAAC
2667	CCCTTTTATATGGTAAAAGACAATATACGTTATAACAACG
2668	ATTGTCTTTTACCATATAAAAGGGGAATATTTGAAAATGA
2789	GATTGGTCATTTTCAAATATTTTTTATATGGTAAAAGACAATATACGTTATAACAACG
2790	GTTGTTATAACGTATATTGTCTTTTACCATATAAAAAATATTTGAAAATGACCAATCC
2906	GTTTCAAAAGGTGAAGAATTATTTAC
3189	TTCTCATTTTTAATTAGTTATAATTAACTAAAATGATACGGGCAAATAGAAAGGAT
3190	AATAATTCTTCACCTTTTGAAACATCTCTCTCAGCTAAAACATCTACAG
3229	ctaaagggaacaaaagctgggtaccATGGTTGTTGAAGTATGGTCTA
3230	CTTGTCGTCATCGTCTTTGTAGTCTTGAATCACCATTTCCGGCT
3231	GACTACAAAGACGATGACGACAAGTAAATGTATAATAAAGATGACGTGTTGAAC
3232	ctcactatagggcgaattggagctcTGTCAATAGCATGTTTAGAATTAAATTAAA

* Plasmids were constructed by isothermal assembly with the indicated PCR product(s) (8). Numbers (#/#) are primer pairs used for PCR amplifications on the indicated substrate. For primer sequences, see Table 1 bottom part.

Figure 1: Computer prediction of IsrR and mutated IsrR pairing with *miaB* mRNA

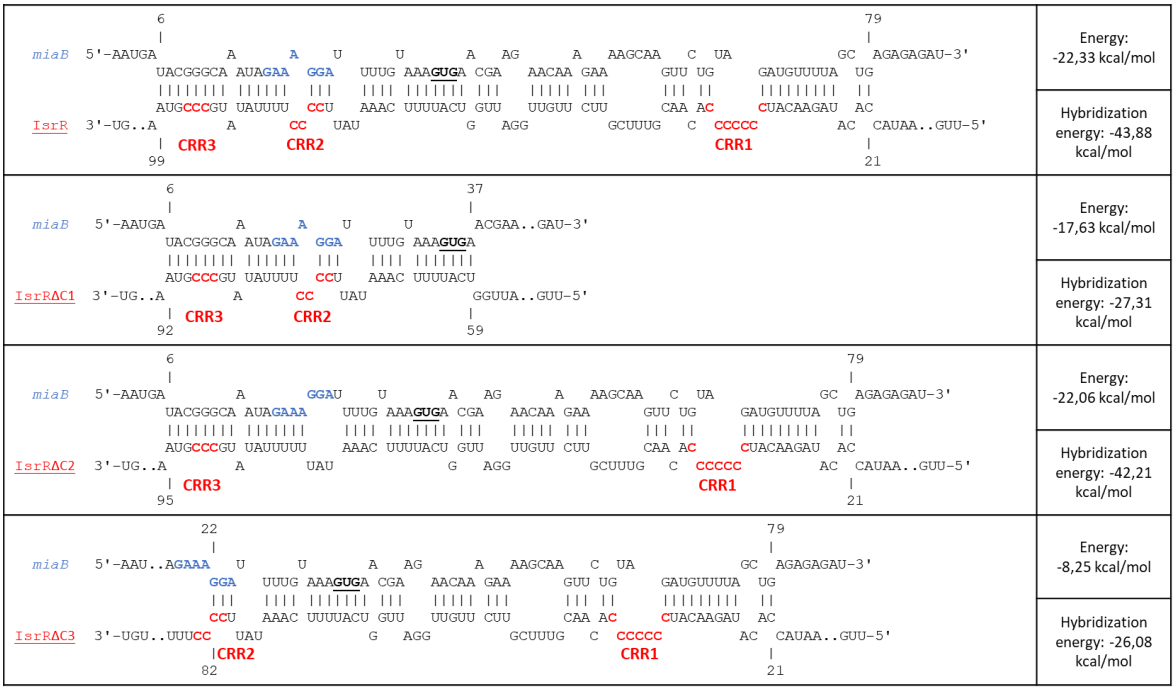

IntaRNA (10) pairing prediction of IsrR and IsrR derivatives deleted for CRR1, CRR2 or CRR3 with *miaB* mRNA. Blue sequences, SD; red sequences, CRRs; bold underline characters, GUG start codon; E, energy; HE, hybridization energy.

Figure 2: MiaB-Flag reporter detection

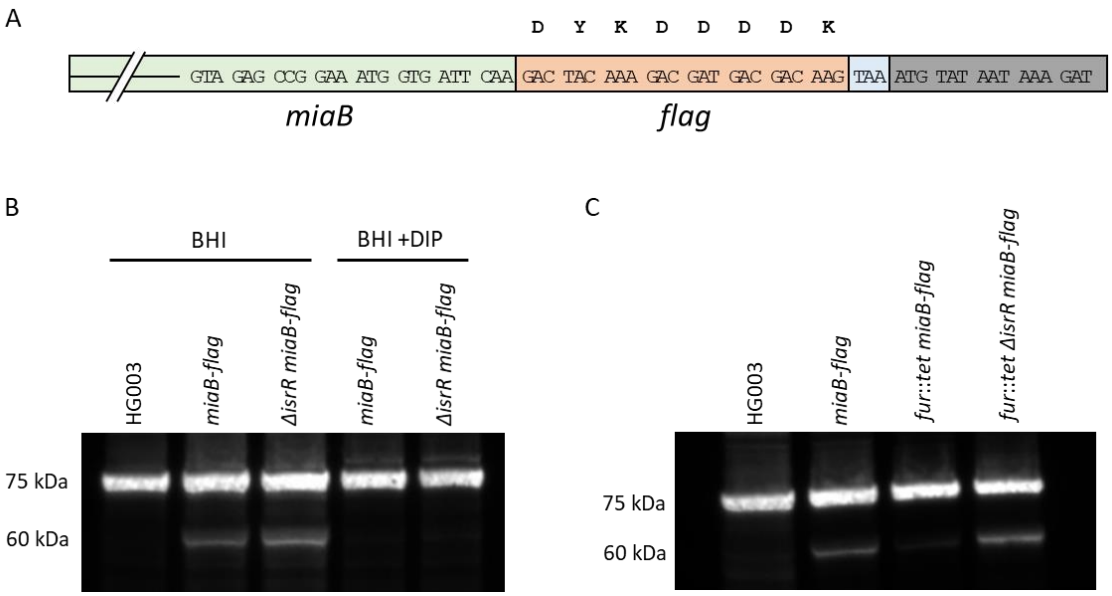

A) Schematic representation of the MiaB-Flag reporter fusion. Green, 3' end of *miaB* ORF; pink, *flag* sequence; blue, native stop codon; grey, first nts of *miaB* 3' UTR. B) Western blot experiment with anti-Flag antibodies in present or absence of iron chelators (n=4). Genotypes and growth conditions are indicated. 75 kDa, non-specific signal present in all samples including Flag-less strain. 60 kDa, signals corresponding to MiaB-Flag. C) Western blot experiment with anti-Flag antibodies with *fur* and *fur*::*tet* strains (n=4) as explained in Figure 2B.

Figure 3: Translational repression of *miaB* reporter fusion by IsrR

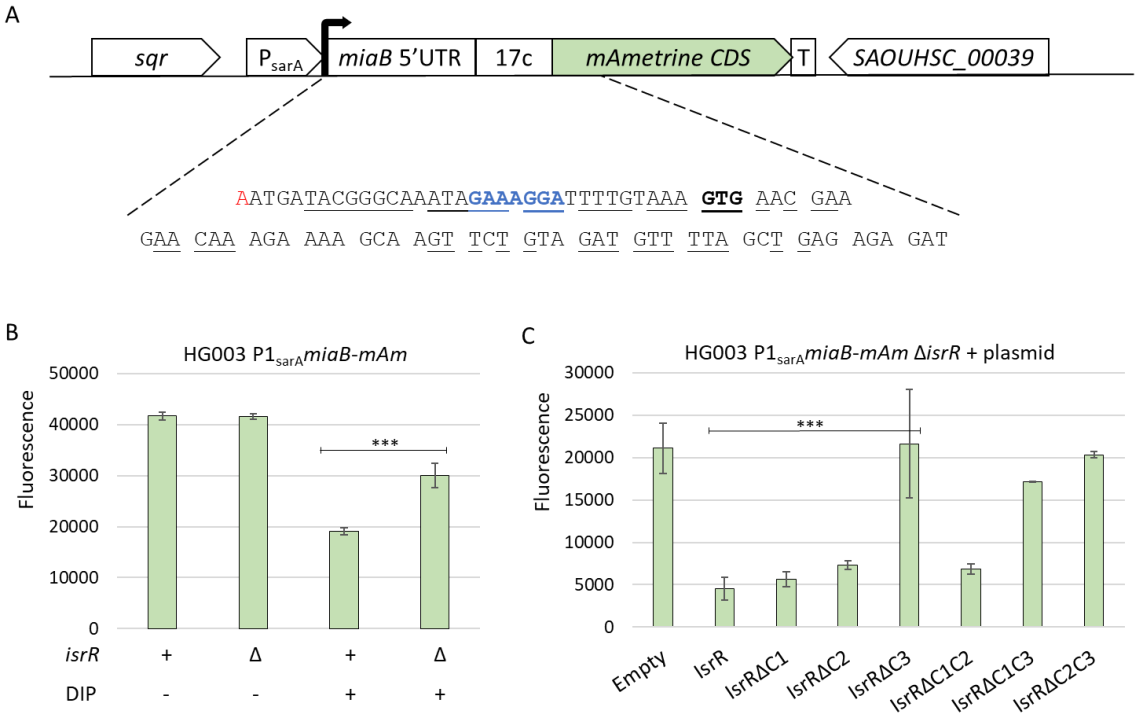

A) Chromosomal reporter fusion for detection of IsrR activity. Red nt; transcription start site, blue bold nts; RBS, black bold nts; start codon, underlined nts; nts in interaction with IsrR as predicted by IntaRNA. B) The translational activity of the *miaB-mAm* reporter fusion was quantified by growing strains HG003 and Δ*isrR* HG003 harboring the fusion on BHI and BHI supplemented with DIP. Results (n=3) are normalized to OD_{600}=1. C) The Δ*isrR* strain harboring the *miaB-mAm* reporter fusion was transformed with plasmids expressing different versions of IsrR and cultured in BHI supplemented with DIP. The translational activity of the reporter fusion was quantified by measuring the fluorescence. Results (n=3) are normalized to OD_{600}=1. **, P-value < 0.01; ***, P-value < 0.001.

Figure 4: Contribution of CRRs to downregulate different mRNA targets

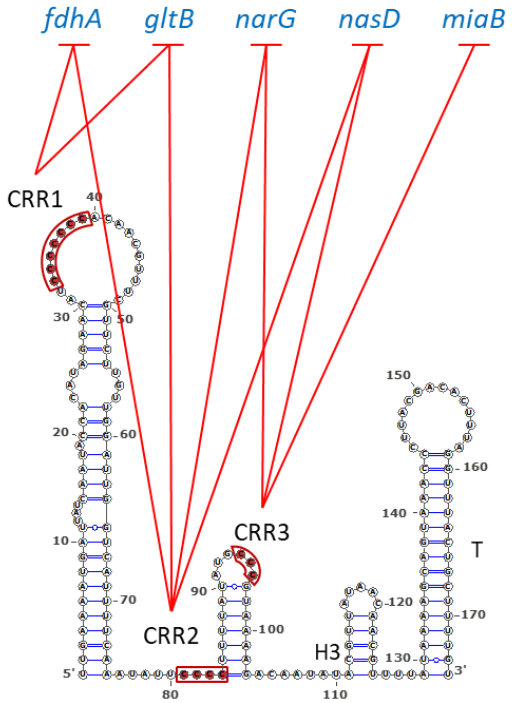

Negative arrows starting for either CRR1, 2 or 3 and pointing to mRNA targets indicate CRRs required for IsrR activity toward the corresponding targets. Data from in vivo results with fluorescent reporters in (3) and this work.